Theor. Appl. Climatol. 76, 219–234 (2003)
DOI 10.1007/s00704-003-0015-6

Theoretical and Applied Climatology
Printed in Austria

[1] Earth Sciences Centre, Göteborg University, Sweden
[2] Department of Physical Geography and Ecosystems Analysis, Lund University, Sweden
[3] National Climate Center, China Meteorological Administration, China

Performance of the Rossby Centre regional atmospheric model in Southern Sweden: comparison of simulated and observed precipitation

C. Achberger[1], **M.-L. Linderson**[2], and **D. Chen**[1,3]

With 7 Figures

Received May 18, 2002; revised April 23, 2003; accepted May 3, 2003
Published online November 17, 2003

Summary

Two climate model simulations made with the Rossby Centre regional Atmospheric model version 1 (RCA1) are evaluated for the precipitation climate in Scania, southernmost Sweden. These simulations are driven by the HadCM2 and the ECHAM4/OPYC3 global circulation models (GCMs) for 10 years. Output from the global and the regional simulations are compared with an observational data set, constructed from a dense precipitation gauge network in Scania. Area-averaged time series corresponding to the size and location of the RCA1 grid points in Scania have been created (the Scanian Data Set). This data set was compared to a commonly used gridded surface climatology provided by the Climatic Research Unit (CRU). Relatively large differences were found, mainly due to the fact that the CRU-climatology uses fewer stations and lacks a correction for rain-gauge under-catch. This underlines the importance of the data set chosen for model evaluations. The validation is carried out at a large scale including the whole area of Scania and at the finest resolution of RCA1 (the grid point level). When integrated over the whole area of Scania, RCA1 improves the shape of the annual precipitation cycle and the inter-annual variability compared to output from the GCMs. The RCA1 control climate is generally too wet compared to the observations. At the grid point level, RCA1 improves the simulation of the variability compared to the GCMs. There is a strong positive correlation between precipitation and altitude in all seasons in the observations. This relationship is, however, much weaker and even reversed in the RCA1 simulations. Analysis of the dense rain gauge network reveals features of spatial variability at around 20–35 km in the area and indicates that a finer resolution is needed if the spatial variability in the area is to be better captured by RCA1.

1. Introduction

Assessments of climate change, related to increasing concentrations of atmospheric greenhouse gases or other perturbations of climate forcing, are primarily based on mathematical and physical models of the climate (Lambert and Boer, 2001). Global Circulation Models (GCMs) are used to simulate the time-dependent evolution of the state of the climate system and can be run with various concentrations of greenhouse gases. Recent GCMs operate on large spatial scales of about 300–500 km, (Mearns et al., 1999) and are able to simulate the large-scale characteristics of the climate. Features that influence the climate on the regional scale (such as topography, land/water distribution or vegetation) are, however, treated in a highly smoothed manner by the GCMs. For many applications related to agriculture, forestry or civil engineering as well as for other impact studies, detailed

climate information at the regional (about 100 km) and local scale (10–50 km) is essential. Thus, various downscaling techniques have been developed to infer near surface climate variables at regional and local scales from the coarse resolution GCM results. These techniques are usually divided into statistical and dynamical downscaling approaches (IPCC, 2001). The latter method makes uses of a high resolution Regional Climate Model (RCM) that is driven by the boundary conditions taken from a GCM. In this way, local forcings and sub-grid scale processes acting on scales smaller than the grid size of the GCM are taken into account resulting in more detailed climate simulations compared to the coarse GCM results (Giorgio and Mearns, 1999). In statistical downscaling, empirical relationships between large-scale climate features and the local climate are used to provide predictions of climate variables at the local scale (Wilby et al., 1999; Busuioc et al., 2001). In Sweden, both downscaling techniques are used for regional climate change scenarios. A RCM has been developed within the framework of SWECLIM (Swedish Regional Climate Modelling Program). This model, the Rossby Centre regional Atmospheric model 1 (RCA1), provides regional climate scenarios at horizontal resolutions of either 88 km or 44 km (Rummukainen et al., 2001; Bergström et al., 2001; Räisänen et al., 2001).

Any model should be evaluated against observations to identify systematic errors and to assess its reliability. A commonly used evaluation approach is to compare simulated fields of climate variables with corresponding observations. Usually, the modeled field consists of a considerable number of model grid points that are merged together prior to the evaluation in order to reduce the model's random ''noise'' at grid point level and to make evaluations representative for a certain geographical region. Examples of model evaluation following this approach may be found in e.g. Christensen et al. (1998) or Noguer et al. (1998). These evaluations normally assess how well simulations reproduce observed spatial patterns of, for instance, air pressure, precipitation or temperature over relatively large areas like Europe.

For practical applications, model output at the finest spatial resolution is provided and used. This raises the question as to what extent the model actually represent the reality at its highest spatial resolution. Evaluation and application of a RCM at the grid box level is sometimes necessary. For example, Christensen and Kuhry (2000) compared grid point values (temperature and precipitation) with point measurements in the Russian Arctic to evaluate high-resolution permafrost simulations. Bergström et al. (2001) used the climate change signal of single RCA1 grid boxes as input for a hydrological model in Sweden. Räisanen and Joelson (2001) compared observed daily maximum precipitation at a number of stations in Sweden with the corresponding variable at the closest RCA1 grid box. Hellström et al. (2001) compared dynamically downscaled precipitation in Sweden using single RCA1 grid boxes with results from statistically downscaled station precipitation and evaluated the model results with station observations.

With the rising awareness about the consequences of climate change on society and environment, the need for highly resolved climate simulations as input to impact studies is increasing. Consequently, the question of what exactly can be expected from a climate simulation at the finest model resolution is becoming more and more important. A natural way to answer this question is to compare simulations with observations at the finest spatial resolution in addition to field comparisons over a region. In this study, this approach is used for precipitation in Scania, southern Sweden. It should be seen as a complement to the previous evaluations of RCA1 regarding its application to extended regions in Europe (e.g. Rummukainen et al., 2001; Räisanen and Joelsson, 2001). The comparison focuses on how well certain features of the precipitation climate are reproduced by RCA1 at its 44 km resolution and over the whole of Scania. More specifically, the study aims are:

a) to identify the dominant spatial scale at which the observed precipitation climate varies in Scania, and to compare this scale with the current resolution of RCA1;
b) to compare observed and modeled precipitation statistics on the grid cell level and over the whole region;
c) to investigate whether dynamical downscaling contributes to more ''realistic'' simulations compared to output from GCMs.

There are a number of motivations for such a study in Scania. First of all, there exists a relatively dense rain-gauge network compared to other regions in Sweden (101 stations cover a region of approximately 100×100 km). The large number of stations allows a reliable estimation of spatially averaged precipitation on a regular grid, matching the size and location of the RCA1 grid boxes. It is expected that this data set (in the following referred to as the Scanian Data Set) represents the spatial variability of precipitation better than other precipitation climatologies with comparable spatial resolution but based on fewer stations. Secondly, a detailed evaluation of RCA1 in Scania is useful because the region is one of Sweden's most important agricultural and most densely populated areas, making the performance of the model an important issue.

2. Models and data

2.1 The RCA1 and the GCM

RCA1 has been developed from the limited area weather forecast model HIRLAM (Källén, 1996) that is in operational use in several European countries. The schemes for soil, snow and the surface were adapted to allow long-term climate runs. Baltic Sea surface temperature and ice are calculated prognostically. The model domain comprises northern and central Europe with a vertical resolution of 19 layers between the surface and 10 hPa and a horizontal resolution of 44 km. Further details on RCA1 can be found in Rummukainen et al. (2001).

RCA1 uses boundary data from the global models HadCM2 (Johns et al., 1997; Mitchell and Johns, 1997) and ECHAM4/OPYC3 (Roeckner et al., 1999; Oberhuber, 1993; Hu et al., 2001), both are coupled ocean-atmosphere GCMs. HadCM2 has a spatial resolution of 2.5° in latitude and 3.75° in longitude, corresponding to about 300 km of spatial resolution at 45° latitude. The model has 19 levels in the atmosphere and 20 in the ocean. At the ocean-atmosphere interface, averaged daily fluxes of heat, momentum, and water are provided to the ocean in a 1-day coupling cycle. The ocean surface temperature and salinity are kept close to a specified seasonally varying reference climatology to prevent the model from drifting towards an unrealistic state. ECHAM4 is based on the European Centre for Medium-Range Weather Forecasts atmospheric model modified for climate studies and it is coupled with the OPYC3 oceanic general circulation model developed by Oberhuber (1993). The model atmosphere consists of 19 levels in the vertical, whereas in the ocean there are 10 layers below the surface-mixed layer. Atmospheric processes are represented in spectral space (T42 truncation) corresponding to a spatial resolution of about $2.8° \times 2.8°$. The atmospheric and the oceanic model are coupled through flux exchanges. ECHAM4 obtains sea surface temperatures from OPYC3 and provides the ocean model with momentum fluxes (unconstrained), heat and freshwater fluxes (adjusted on annual averages). According to the land-sea mask of both GCMs, the area of Scania is located within a sea grid box. For climate change experiments RCA1 is fed with time slices covering periods of 10 years with one time slice acting as control period and the other one as scenario period (climate under increased greenhouse gas concentrations). There are differences in the control climate of both the GCMs with respect to the assumed radiative forcing: in HadCM2 the equivalent CO_2 concentration is kept constant on a pre-industrial level until 1990, whereas in ECHAM4/OPYC3 the equivalent CO_2 concentration increases by roughly 30% between the beginning of the run and 1990. In each case, the control climate time slices for driving RCA1 are centered around 1990 (Rummukainen et al., 2001). To date, there is only one decade-long RCA1 control run available for each of the GCMs. Therefore, these should be considered as just one example and may not be representative of other realizations. The focus of this study is on the control climate runs from HadCM2 and ECHAM4/OPYC3, together with their RCA1 runs H-RCA1 (driven by HadCM2) and E-RCA1 (driven by ECHAM4).

2.2 The precipitation gauge network in Scania

The analysis is performed on 101 monthly series, which are based on daily precipitation measurements between 1963 and 1990 with a station density of 1 station/100 km^2. The dense rain-gauge

network was obtained by combining a regional network of daily measurements, the 'Ellesson dataset' (Ellesson, 1993) with precipitation measurements made by SMHI (Swedish Meteorological and Hydrological Institute). The 63 stations of the Ellesson dataset were equipped with the SMHI standard rain gauges and observations were made at standard time. Less than 10% of the data were missing in each series, except for a few stations located in areas with low station density. Missing data have been interpolated according to a method developed by Alexandersson and Moberg (1997). A missing value is interpolated from a mean of all surrounding stations where all stations are assigned a weight, depending of the correlation between this station and the station with the missing values. The precipitation series were homogenised by the Standard Normal Homogeneity Test (SNHT), developed by Alexandersson and Moberg (1997) and implemented by Steffensen (1996). Corrections were made to stations with significant inhomogeneity, but only if the inhomogeneity could be associated with known changes, e.g. relocation of instrumentation or equipment changes.

As discussed by Osborn and Hulme (1997), observed station statistics are not readily comparable with the modeled grid-box means, as the

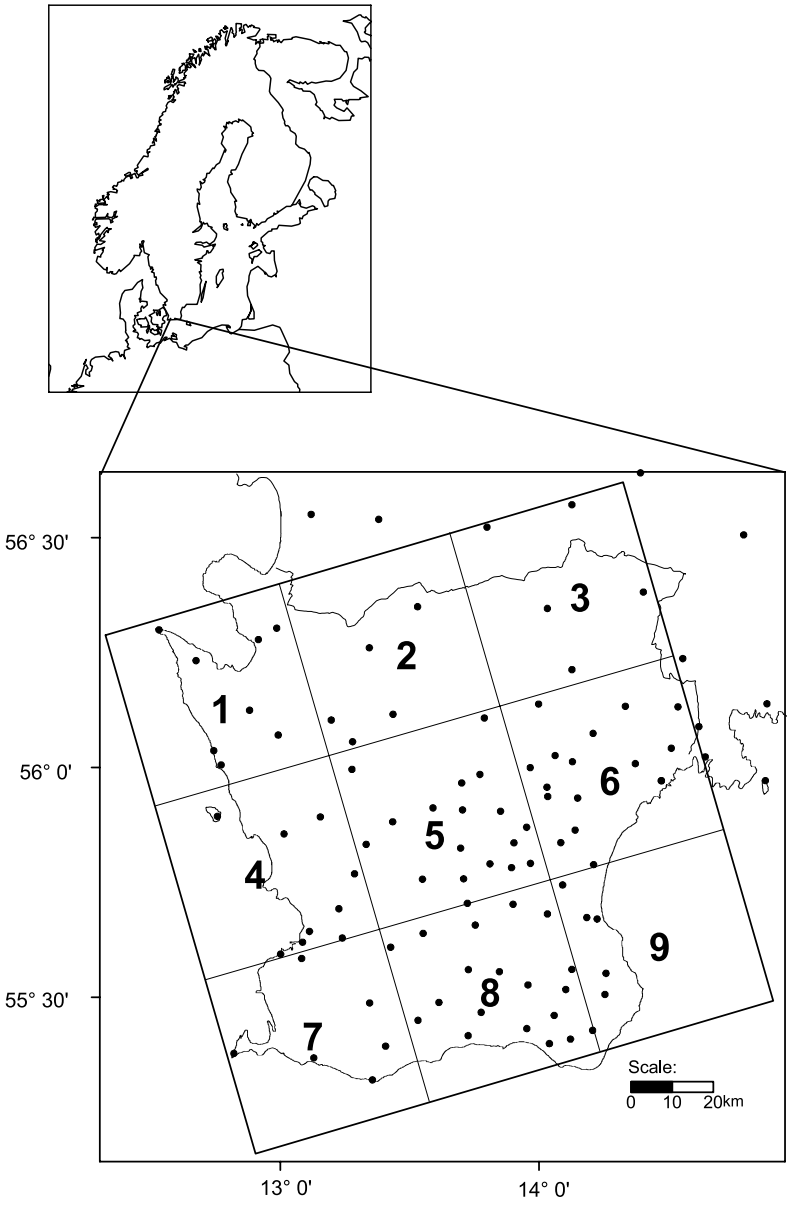

Fig. 1. Location of the RCA1 grid boxes in Scania and their numbering. The dots show the location of the station used for evaluation

distribution from a single station time series will be more skewed than a grid-box mean. This will mainly affect the variance and thus the comparison of standard deviations between observed and modeled data. If more stations are averaged, the skewness of their mean precipitation time series decreases and variance is reduced. With increasing numbers of stations, the variance is reduced more slowly. The decrease of the variance is dependent on the mean interstation correlation between all pairs (Osborn and Hulme, 1997) and thus varies with investigation area. This method was used to evaluate the number of stations needed in Scania to make the observed and modeled precipitation statistics comparable. To account for differences in paired correlations in different parts of the landscape, the minimum paired correlation in the area was used in the computations. The reduction in variance changes quickly up to five stations and then levels off. The asymptotic variance corresponds to about 90% of the variance and 95% of the standard deviation of the five-station mean series. The number of stations used in this study is thus considered sufficient for comparing observed and modeled grid-box means.

The station precipitation series were interpolated into areal mean values corresponding to the RCA1 grid-cells. Figure 1 shows the location of the nine RCA1 grid cells in Scania. As the stations are unevenly distributed within the grid-cells, each station was assigned a weight corresponding to the area represented by the station. These weights were estimated by Thiessen polygons to calculate monthly time series, one for each RCA1 grid cell.

Observed precipitation is affected by a number of measurement errors resulting in an underestimation of the actual amounts compared to the measured precipitation. Losses due to the wind field deformations around the gauge, the wetting of the inner walls of the collector and evaporation of rainwater from the gauge are common. During winter, blowing and drifting snow adds further uncertainty to the measurements (Rubel and Hantel, 2001). For Swedish conditions the actual annual precipitation is expected to be about 15% higher than the precipitation measured with SMHI standard rain gauges (Raab and Vedin, 1995). This number is in good agreement with findings of Rubel and Hantel (2001) giving an averaged correction factor of 13% when establishing their daily precipitation climatology over the Baltic Sea Experiment (BALTEX) area. Here, the monthly correction factors from Raab and Vedin (1995) were used to establish individual correction factors for the nine RCA1 grid cells. For the analysis of the major spatial scales of precipitation variability described in Section 3.2, an extended station network was used, comprising the Ellesson data set and the SMHI stations. Altogether there are 178 stations with daily measurements between 1974 and 1990 in the area (Linderson, 2003).

3. Precipitation climate in Scania

3.1 General feature

Scania is situated in the southernmost part of Sweden and corresponds to an area of about $10^4\,km^2$ (Fig. 1). The landscape is undulating with low ridges extending in SE–NW direction up to around 200 m above sea level. The southwestern area is dominated by agriculture while the northeastern part consists mainly of forests. Scania lies in the zone of prevailing westerlies and the area has a maritime climate classified as humid, warm temperate according to the Köppen climate classification (Ahrens, 1994). The area is affected by cyclonic activity throughout the year with maximum activity during winter when the temperature contrasts between the tropical and polar air masses are greatest. Precipitation is mainly caused by cyclonic activity, although during summer convective processes contribute significantly to precipitation.

3.2 The major spatial scale of precipitation variability

The spatial scale provides information on how strongly a climate variable varies in space and is thus a measure of its spatial continuity. Here, correlograms are used to describe the observed spatial variability and scale in terms of correlating time series between all possible pairs of stations. It describes the decay of correlation with separation distance and is related to the semivariogram (see e.g. Isaaks and Srivastava, 1989). The correlogram is, however, easier to analyse compared to the semivariogram and it

gives a physical meaning (Bacchi and Kottegoda, 1995). The major scale of the spatial variability equals the separation distance at which the correlation is insignificant and is a measure for the range of influence. The correlogram level corresponding to the distance at which values between station pairs are independent is called the sill. Depending on the shape of the correlogram, the practical range corresponds to a value of 64–100% of the sill (Clarc and Harper, 2000).

To produce semivariograms and correlograms that are valid for the whole area, homogeneity in the mean and variance of the dataset is required (Clarc and Harper, 2000). Thus, the area was divided into sub-areas and the difference in mean and variance between the sub-areas were checked and found acceptable. Division into four sub-areas allowed the analysis of the east–west and south–north differences and the number of observations was sufficient to make the statistics meaningful.

The correlation decay is evaluated for a certain distance, the so-called lag distance. Here, a lag distance of 10 km is used as it gives a good resolution of the distance as well as a sufficient amount of pairs for each lag distance. Both omni-directional and directional correlograms are used. The first type shows the mean decay of the correlation for all directions, while the latter shows the change of correlation in a specified direction. Directional correlograms are produced for 16 sectors with 22.5° each.

One of the most important factors that determine the spatial variability of climate variables is topography. It also strongly influences the regional precipitation variability in Scania (Linderson,

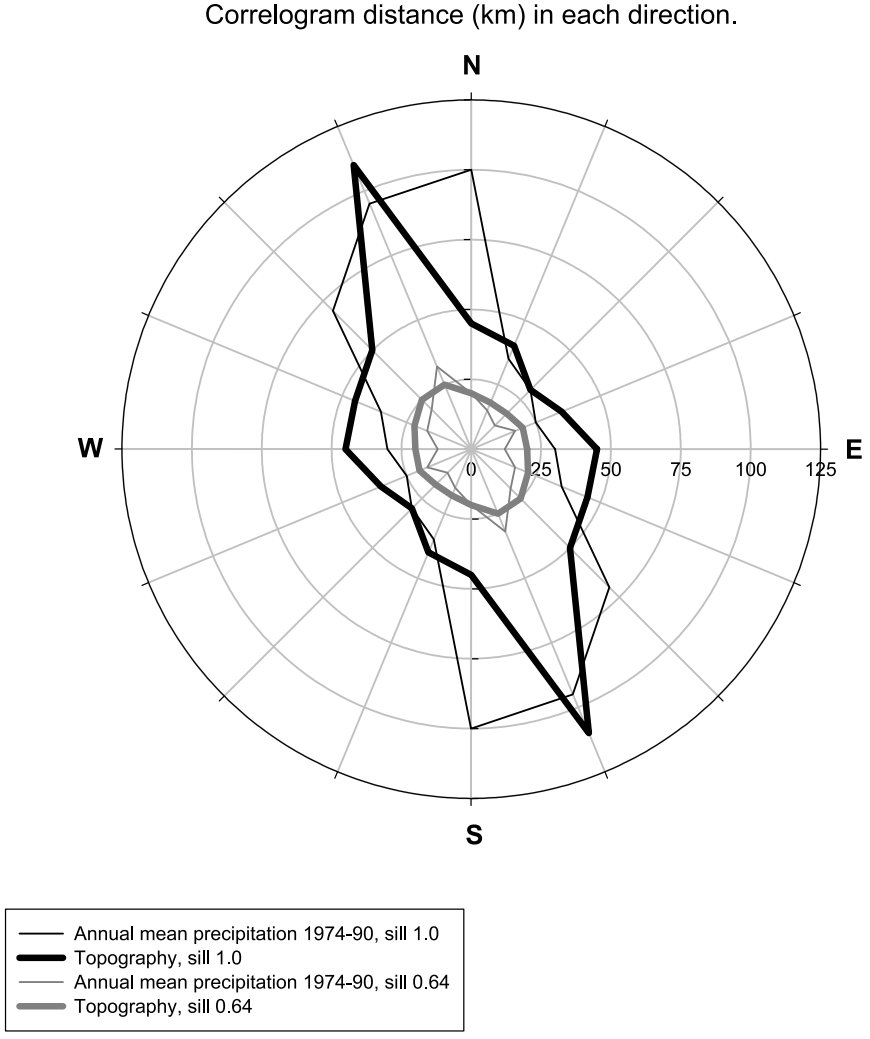

Fig. 2. Correlogram for topography and annual mean precipitation. Two different values for the sill have been used

2003). To illustrate this, correlograms of the spatial variability of the topography are included in Fig. 2. These correlograms were obtained using height data for Scania from a Digital Elevation Model (DEM) with a spatial resolution of 500 m originating from the Swedish National Land Survey. To decrease the number of points included in the analysis, the DEM was interpolated to obtain a coarser spacing of 4000 m between grid points.

The omni-directional correlogram range for annual precipitation is 20 km for the sill value 0.64. This indicates that the RCA1 resolution (grid size $44 \times 44\,\mathrm{km}^2$) is generally too coarse to match the major scale of precipitation in the area. Even with a sill value of 1.0 the range (35 km) shows that the RCA1 resolution is insufficient. The range varies with direction and has an elongated shape in the N–NW to S–SE direction, especially for the 1.0 sill value (Fig. 2). This

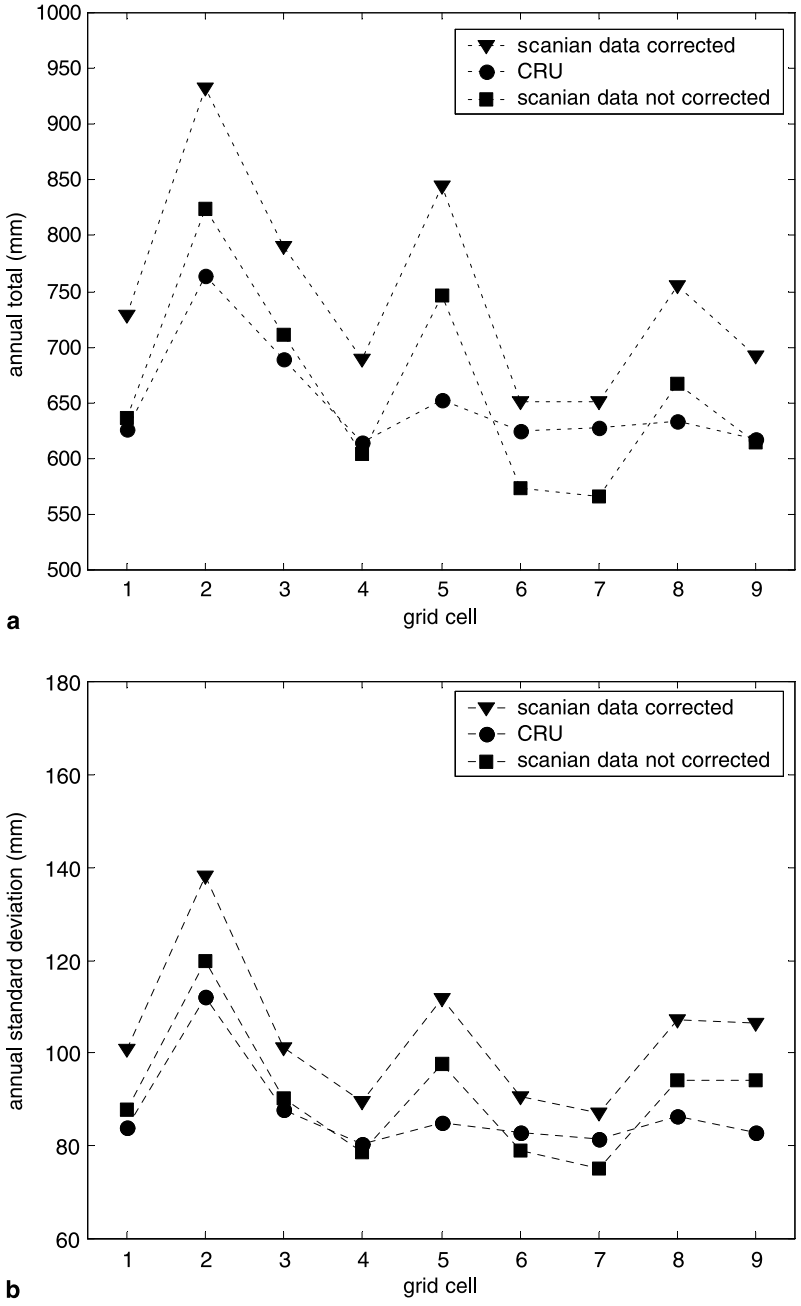

Fig. 3. Comparison of CRU-data with the Scanian Data Set before and after the correction for rain gauge under-catch, **a** annual totals, **b** annual standard deviation for each grid cell

is in accordance with the spatial variability of the topography, but the correlograms for precipitation show a slight deviation towards N–S direction compared to topography, that could be due to the influence of the distance to coast. A similar complex influence of the physiography on the shape of the semi-variogram is found for England, although topography is the major factor contributing to the scale of the annual precipitation variability (Bigg, 1991).

Multiple linear regression was used to detrend the annual precipitation amounts for the influence of topography and distance to coast. The 0.64 and 1.0 sill values of the omni-directional correlogram of the detrended precipitation occur at the same distance as for the non-detrended precipitation. After detrending, the directional correlograms show a slightly elongated shape in the SW–NE direction. This confirms a trend of increasing precipitation with height, distance to coast and from SE to NW as discussed by Linderson (2003).

3.3 The Scanian data set compared to the CRU-climatology

The precipitation climatology compiled at the Climatic Research Unit, University of East Anglia, UK (in the following named CRU-climatology) is frequently used for climate model validation (e.g. Rummukainen et al., 2001; Christensen et al., 1998; Noguer et al., 1998). The CRU-climatology has a spatial resolution of 0.5° latitude by 0.5° longitude and has been interpolated directly from observations using thin-plate spline functions with elevation, latitude and longitude as predictors (New et al., 1999, 2000). Since the geographical position of the grid points over Scania in the CRU-climatology deviates from the location given by the RCA1 grid, the CRU data has been interpolated to the latter grid to avoid biases in the comparison due to differences in grid size and location.

Figure 3a and b show annual totals and standard deviation for the CRU data and the Scanian Data Set. On annual scales, both data sets show a similar geographical precipitation distribution with larger annual totals and variability in the central part (grid cells 2, 5 and 8) and lower values in the southern region. The CRU data is not adjusted for rain gauge under-catch (New et al., 2000), which explains the bigger differences between the CRU data and the Scanian data set that is corrected for under-catch. Further, the CRU climatology has a systematically lower variability between grid cells than the Scanian data. The orographic precipitation enhancement, obvious in the Scanian Data set (grid cell 2, 5 and 8), is much weaker in the CRU data. The main reason for this finding is presumably the lower station coverage of the CRU data. Frei and Schär (1998) report similar results when comparing precipitation fields in the Alps obtained from high-resolution rain-gauge observations with the CRU data set. They concluded that coarse-resolution global data sets are designed for validating global climate models at the 100–200 km scale, rather than for regional climate models at higher resolution.

4. Comparison of observed and modeled precipitation

This section addresses the skill of the regional model in reproducing the annual cycle of precipitation, the frequency distribution, the spatial pattern, and the relationship between topography and precipitation found in the observed data. All comparisons regard observed and simulated precipitation *climates*. This is due to the nature of the climate simulation of GCMs and RCMs. The comparison is done for the nine grid boxes and for the whole area including all the grid boxes.

4.1 The seasonal cycle in the GCM, RCA1 and the observations

The seasonal cycle of precipitation is an important climate property and should be realistically reproduced by models that are used in applications related to water availability. Differences between the observed and modeled seasonal cycle may also help to reveal systematic errors in a model. Here, the seasonal cycle is examined using two different spatial resolutions. In the first case, spatial averages for the whole area are made from the nine grid points for observed and simulated data. In the latter case, the seasonal cycle of the nine grid cells are examined individually.

4.1.1 Scania as one grid box

Data from the GCMs, the RCA1-runs and the observations had to be made comparable in terms of spatial resolution and coverage. The GCM data were therefore interpolated to an area corresponding to the nine RCA1 grid cells (size about $1^\circ \times 1^\circ$) with the area's center located at 55.9° N, 13.55° E. For the observations and the H-RCA1 and E-RCA1 data, spatial means over the nine grid cells were computed.

At this larger scale, the seasonal cycles of HadCM2 and H-RCA1 (Fig. 4a) are in good agreement in spring but HadCM2 does not capture the precipitation maximum in summer. ECHAM4 deviates strongly from the observations throughout the whole year, and the seasonal cycle is almost reversed to the observed seasonal cycle. These differences are most likely a consequence of the GCM land-sea mask that assigns the grid point as sea. E-RCA1 produces a more realistic cycle but the monthly precipitation

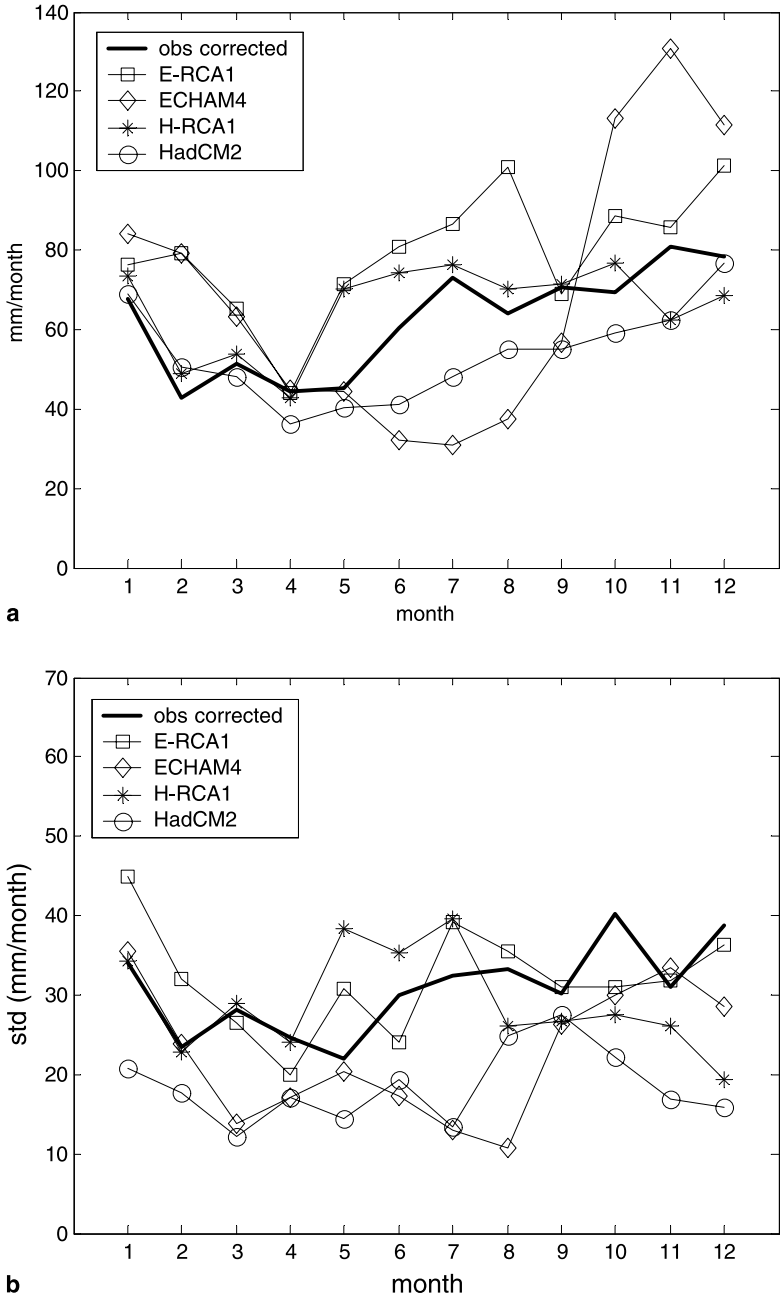

Fig. 4. a Seasonal cycle of precipitation (monthly totals) for HadCM2, H-RCA1, ECHAM4, E-RCA and the observations; **b** same as a) but for monthly standard deviation

Table 1. Student's T-test applied on seasonal totals obtained from GCM, RCA1 and observations. Differences significant at the 5%-level are indicated by '*', insignificant deviations by '–'

Data sets	Winter		Spring		Summer		Autumn	
	HadCM2	ECHAM4	HadCM2	ECHAM4	HadCM2	ECHAM4	HadCM2	ECHAM4
GCM-RCA	–	–	–	–	*	*	–	*
GCM-obs	–	*	–	–	*	*	*	*
RCA-obs	–	–	–	*	–	*	–	–

values are generally too high. The correlation coefficients between the observed and the simulated seasonal cycle are 0.73 for HADCM2 and 0.5 for ECHAM4. The Student's T-test (Table 1) shows significant differences between the observations and the GCMs in summer and autumn (both GCMs) and winter (only ECHAM4). The differences are clearly reduced in H-RCA1 but significant differences remain for E-RCA1 in spring and summer. The seasonal cycle of the observed mean inter-annual standard deviation of monthly means (Fig. 4b) is weak and follows the annual trend of the mean, but this pattern is only partly reflected in the RCA1 runs. The GCM-variability is mostly lower than the observed, probably caused by the coarse GCM resolution and the unrealistic surface for this area. The results found here are in line with model evaluation studies carried out for larger regions. Murphy (1999) compared monthly means and inter-annual standard deviations of precipitation from a GCM, a RCM and observations in Europe and he found that the variability was strongly increased in the RCM compared to the GCM due to increased spatial resolution. Jacob (2001) compared annual cycles of observed and simulated precipitation over land surfaces within the Baltic Sea drainage basin with the regional climate model REMO driven by ECHAM4/T106. REMO improved the seasonal cycle compared to the driving GCM but resulted in an overestimation of precipitation.

4.1.2 Comparison on the RCA1 grid level

The annual cycles from the different sources were further evaluated at the RCA1 grid level. RCA1 output at single grid points was compared

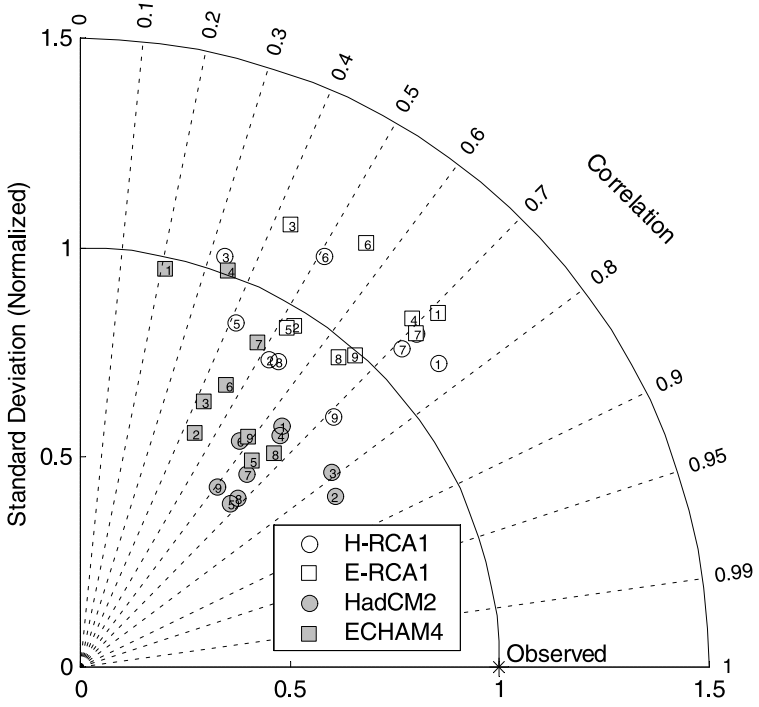

Fig. 5. Taylor-diagram for the H-RCA1 and E-RCA1 grid boxes (white symbols) and HadCM2 and ECHAM4/OPYC3 bilinearly interpolated to the center of the nine grid boxes (shaded symbols). The numbers indicate the location of the grid boxes according to Fig. 1

with GCM data that was bi-linearly interpolated to the centre of each RCA1 grid point (the latter can be considered as a simple downscaling technique). The observed annual cycles of the individual grid boxes (not shown here) are similar to the observed cycle for the $1^\circ \times 1^\circ$ area. The results are summarized in the Taylor-diagram of Fig. 5. The Taylor-diagram gives the correlation between observations and simulations as the azimuthal angle from the origin and the normalized standard deviation (modeled divided by observed) as the radial distance from the origin. The observations are represented as a point at unit distance from the origin along the abcissa with unit correlation and unit normalized standard deviation. Simulations that perform well are thus close to the reference point (Taylor, 2000). Whether the higher spatial resolution of the RCA1 brings an improvement compared to the bi-linearly GCM output depends on the particular model and grid point. It further depends on whether the shape of the annual cycle is considered (as expressed by the correlation) or the variability (as given by the normalized standard deviation). In general, the variability simulated by RCA1 is closer to the observations. All in all, E-RCA1 performs better than H-RCA1.

Hellström et al. (2001) compared the observed seasonal cycles of four stations in Sweden with seasonal cycles from both RCA1 runs and the driving GCMs, the same GCMs as used in this study were used but none of the selected stations was located in Scania. In contrast to our findings here, H-RCA and E-RCA clearly improved the shape of the seasonal cycles. This indicates the difficulty for RCA1 to realistically simulate the regional precipitation climate in southern Sweden. A higher resolution simulation may improve the results.

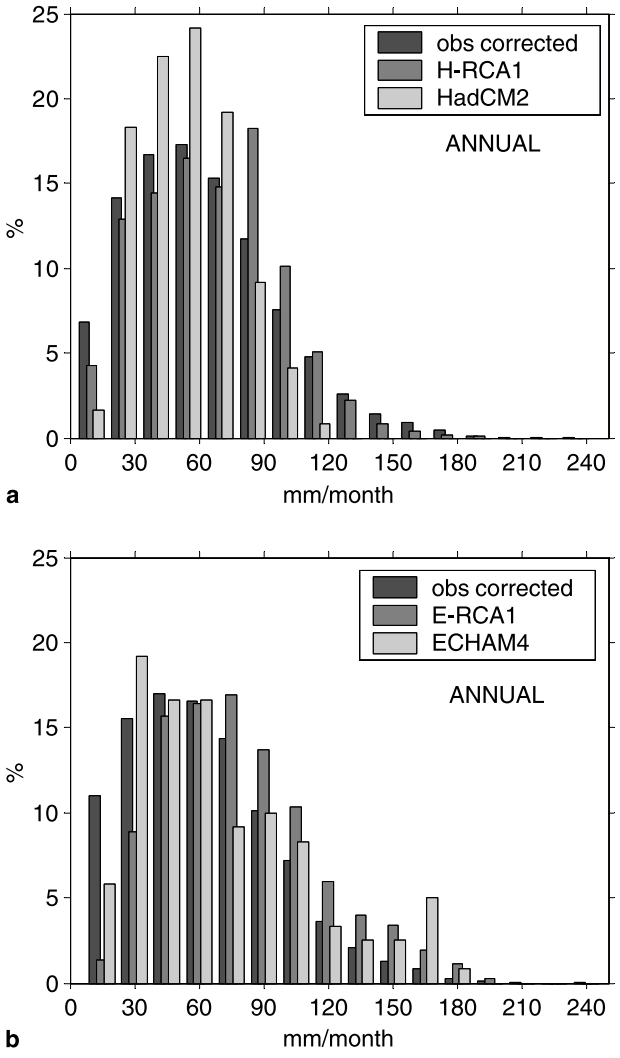

Fig. 6. Frequency distribution of annual precipitation for **a** for HadCM2, H-RCA1 and observations, **b** for ECHAM4/OPYC3, E-RCA1 and observations

4.2 Frequency distribution of precipitation

Another interesting feature of the precipitation climate is the frequency distribution of the precipitation intensity and its representation in the GCMs and RCA1. Figure 6 displays bar charts of the observed frequency distribution together with the simulated distributions for RCA1 and the GCMs. In HadCM2 precipitation intensities in the intermediate ranges dominate (Fig. 6a) but H-RCA1 tends to shift precipitation towards higher intensities, which is probably an effect of its higher spatial resolution. ECHAM4 and E-RCA1 both cover the whole range of classes but intensities $>115\,\mathrm{mm/month}$ are overestimated especially by E-RCA1. All simulations capture low frequencies ($<30\,\mathrm{mm/day}$) poorly. The positive bias in both RCA1 runs (especially E-RCA1), appears to be linked to the overestimation of the frequency of large precipitation amounts.

4.3 The spatial structure in the observations and RCA1

The skill of RCA1 to reproduce the geographical distribution of observed precipitation (corrected)

Table 2. RMSE, bias and the pattern correlation between the observations, H-RCA1 and E-RCA1. '*' indicates significant correlation at 5% level

Season	H-RCA1			E-RCA1		
	RMSE (%)	bias (%)	pattern corr.	RMS (%)	bias (%)	pattern corr.
Winter	13.4	0.8	0.4	35.8	33.2	0.4
Spring	21.3	18.3	0.3	28.8	27.2	0.7*
Summer	17.3	11.9	0.6	37.3	35.5	0.7*
Autumn	15.4	−4.8	−0.4	18.4	10.9	−0.4
Annual	12.4	5.4	0.4	28.1	26.2	0.5

Table 3. Student's T-test performed on seasonal precipitation means for the corrected observations, H-RCA1, and E-RCA1. Differences significant at the 5% level are indicated by '*', insignificant deviations by '–'. The last row (column) shows the number of significant differences in % for each season and model run (grid box)

Grid cell	Winter		Spring		Summer		Autumn		%	
	H-RCA1	E-RCA1	H-RCA1	E-RCA1	H-RCA1	E-RCA1	H-RCA1	E-RCA1	H-RCA1	E-RCA1
1	–	*	–	*	–	*	–	*	0	100
2	–	–	–	–	–	*	*	–	25	25
3	–	*	–	*	–	*	–	–	0	75
4	–	*	–	*	–	*	–	*	0	100
5	–	–	–	–	–	*	*	–	25	25
6	–	*	*	*	*	*	–	*	50	100
7	–	*	–	*	*	*	–	*	25	100
8	–	–	–	–	–	*	–	–	0	25
9	–	–	–	–	–	–	–	–	0	0
%	0	55	11	55	22	89	22	44		

statistics at grid cell level is analyzed in this section. Table 2 gives the pattern correlation here used as a measure of the agreement between observations and simulations in their spatial patterns, the Root-Mean-Square Error (RMSE) and the bias. RMSE and bias are in general higher for E-RCA1 than for H-RCA1. According to the pattern correlation, however, E-RCA1 and observations are in better agreement compared to H-RCA1. For both models the pattern correlation is negative in autumn, this is more closely examined in Section 4.4. Differences for the grid points have been tested for their statistical significance using the Student's T-test on time series of seasonal totals (Table 3). With H-RCA1, fewer grid points differ significantly compared to E-RCA1, indicating that the H-RCA1 modeled precipitation amounts are in better agreement with the observations.

In the RCA1 evaluation by Rummukainen et al. (2001), a general positive precipitation bias is mentioned for RCA1. Values of 16% (H-RCA1) and 28% (E-RCA1) are given for the Nordic region (Norway, Sweden and Finland). The reason for the higher bias in E-RCA1 is, according to the authors, likely to be due to differences in the atmospheric circulation and the temperature/humidity produced by H-RCA1 and E-RCA1. It is obvious that these factors may have also played a role in creating the difference in the simulated precipitation over Scania.

4.4 The relationship between precipitation and topography

The correlation between precipitation and orography is often examined to demonstrate the improvement of precipitation distribution achieved by a climate simulation at higher resolution compared to the GCM simulation (e.g. Noguer et al., 1998; Rummukainen et al., 2001). Here, the relationship between height and precipitation is studied for the nine grid

boxes of Scania. Precipitation is usually enhanced by orography, mainly due to the forced uplift of air. Factors that influence the amount of the orographic precipitation are air mass characteristics, synoptic-scale pressure patterns, and local motion induced by the terrain (Barry, 1992). For Scania, earlier studies show that the spatial precipitation distribution is highly connected to topography (Linderson, 2003). The height data used for the correlation with precipitation observations was obtained from a DEM provided by the National Land Survey of Sweden. Each grid cell height was estimated as the mean value of all DEM points within the grid cell although, excluding DEM points located in the sea, since all gauges used here are located on the Swedish mainland. For the models, the height information was taken from the RCA1 topography. Both the model topography and the DEM derived grid box heights reflect the elevated part of central Scania, although the RCA1 heights are generally lower than the DEM data. Coastal grid boxes have lower heights in the model topography than in the DEM derived topography. The difference is biggest for grid point 9 (the south-east corner) as a large fraction of that box is located in the sea.

Figure 7 and Table 4 show that the relation between precipitation amount and altitude is stronger in the observations compared to H-RCA1 and E-RCA1. This is indicated by the steeper slope of the regression line and the higher value of the correlation coefficient r for the observations (column 8 of Table 4) compared to the models (column 4, 7 of Table 4). The observed height-precipitation relationship is positive for all seasons. For H-RCA1 and E-RCA1, however, r is negative in autumn, a feature already mentioned earlier (see Table 2). To reveal the possible causes for the negative correlation in autumn, seasonal values for r were calculated separately for the modeled large-scale precipitation as well as for the modeled convective precipitation. Since the convective fraction of the observed precipitation is not known, this analysis could only be done for the model output. The convective part amounts for H-RCA1 to 4% (DJF), 15% (MAM), 55% (JJA), 38% (SON) and 28% (ANN) of the total precipitation. The corresponding numbers for E-RCA1 are 3% (DJF), 18% (MAM), 45% (JJA), 27% (SON) and 24% (ANN). There is also a general agreement between E-RCA1 and H-RCA1 in terms of the relationship between convective precipitation and height. While summer (JJA) and spring (MAM) show a positive correlation, winter (DJF) and autumn (SON) display a reversed relationship. This is not surprising as the convective

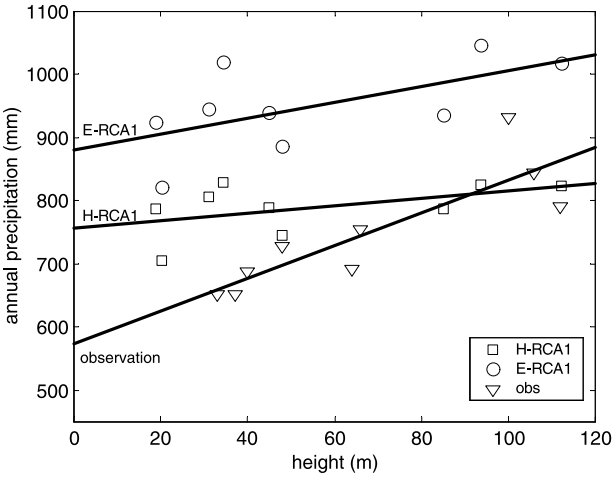

Fig. 7. Relationship between annual precipitation totals and grid box height for the observations and the RCA1

Table 4. Correlation coefficients for seasonal and annual precipitation totals vs. height for the RCA1 and the observations. For H-RCA1 and E-RCA1, the correlations are given for the convective and the large-scale precipitation separately as well as for the total (convective + large-scale) precipitation. The stars indicate significant correlation at the 5% level

Season	H-RCA1			E-RCA1			obs
	large scale prec.	convective prec.	total prec.	large scale prec.	convective prec.	total prec.	
DJF	0.5	−0.5	0.4	0.5	−0.5	0.5	0.9*
MAM	−0.1	0.9*	0.7*	0.6	0.9*	0.8*	0.9*
JJA	0.7*	0.4	0.5	0.7*	0.6	0.6	0.7*
SON	0.7*	−0.9*	−0.7*	0.8*	−0.9*	−0.5	0.8*
ANN	0.8*	−0.2	0.5	0.8*	−0.2	0.6	0.8*

precipitation is determined by the parameterization scheme of RCA1. For large-scale precipitation, the only difference between the two model setups appears in spring when H-RCA1 has a weak negative relationship between the precipitation and height while E-RCA1 shows a positive correlation. This difference is presumably due to differences between the driving GCMs. If this is true, then E-RCA1 may present a better combination of regional and global models for this region than H-RAC1. It is clear that the negative correlation for convective precipitation provides a possible explanation as to why the total precipitation in autumn is negatively correlated with altitude.

Topography clearly influences the observed precipitation in all seasons (Fig. 7). Annual gridded precipitation increases by 2.5 mm/m, whereas the seasonal values vary between 0.4 mm/m in MAM and 0.6 mm/m (SON, DJF). These numbers, however, should be treated with care as they are based on only a few values. Calculating the orographic enhancement from corrected station precipitation, the annual increase amounts to 1.5 mm/m when all 101 stations included in this study are used, or to 1.8 mm/m when the calculation is based on all available gauges in Scania. The numbers are generally in agreement with the overall rainfall-altitude relationship reported for Southern Sweden with 0.5–2.0 mm/m depending on the location with respect to coast (Raab and Vedin, 1995). For Denmark, this figure is 1.6 mm/m calculated from 243 corrected stations originating from Frich et al. (1997). In Great Britain, the precipitation increase with height is 2.4 mm/m varying by region from almost 0 up to 4.5 mm/m, (Brunsdon et al., 2001).

5. Concluding remarks

This study focused on evaluating the 44 km version of RCA1 with respect to the model's performance in reproducing some selected features of the precipitation climate in Scania, a small subarea of the RCA1 model domain. For the comparison, two different spatial scales were applied: precipitation statistics averaged over the 3×3 RCA grid points were compared with the corresponding averaged observed statistics, as well as with the precipitation from two different driving GCMs for the grid point located over Scania. Further, the RCA1 precipitation climate of the individual grid points was compared to observations and bi-linearly interpolated GCM data. The study was restricted to Scania since there exists a relatively dense precipitation network for this region which is useful to derive reliable spatially averaged precipitation statistics.

Data from the Scanian network was gridded to the RCA1 resolution and compared with the well-established CRU-climatology. This comparison showed that the CRU-climatology systematically underestimates the mean and the spatial variability. Clearly, the choice of the data set for evaluation purposes has a strong influence on the outcome of the validation and should be carefully considered in model evaluation exercises. This is especially true for validations that include second-order statistics. The differences between the CRU-climatology and the Scanian Data Set are most likely due to the lower station density of the CRU data and the fact that no under-catch correction is applied.

The spatial scale of rainfall variability in Scania has been estimated to be about 20–35 km and it is closely related to the influence of topography which varies over a similar length scale. Compared to the current RCA1 resolution of 44 km, the observed precipitation thus varies at a scale slightly less than the model resolution, which implies that the current grid cell size is too coarse to fully represent the observed spatial variability. Further, the model reliability is generally lower at the grid point scale compared to a spatial average over a number of grid points, which implies that a finer model resolution would be necessary to satisfactorily resolve the spatial precipitation statistics for Scania.

When comparing the RCA1 simulated seasonal cycle of precipitation averaged over the nine RCA1 grid points it could be shown that dynamical downscaling by means of RCA1 improves the agreement with observations with respect to seasonal totals. However, the higher resolution does not remove the differences in the shape of the annual cycle. At the level of individual grid points, RCA1 strongly enhances the amplitude of the seasonal cycle (the month-to-month variability), but there is no clear improvement with respect to the course of the annual cycle. The large deviations between the seasonal cycles in

the driving GCMs compared to the observations are probably due to the fact that Scania is located in the sea according to the coarse GCM resolution. This might also be the reason why the GCMs lack enhanced summer precipitation, which is more realistically captured by the RCA1 simulations although it is too high and starts too early compared to the observations. The RCA1 seasonal and annual grid cell totals exceed the observed amounts, with E-RCA1 having the more pronounced wet bias.

It was found that the spatial structure of the observed precipitation is not very well captured by RCA1, especially in autumn. Even though the landscape is rather flat and homogeneous (the highest altitude is about 200 m above sea level), there is a strong positive correlation in the observations between precipitation and altitude in all seasons. The relationship is, however, much weaker and even reversed in the RCA1 simulations, which points out that there is potential to improve the regional climate model.

Acknowledgements

The SWECLIM Programme funded by MISTA and SMHI made this work possible. Further, the authors want to thank Karin Larsson for kindly and patiently assisting with the GIS-applications. Cecilia Hellström is acknowledged for reading and commenting on the manuscript.

References

Ahrens CD (1994) Meteorology today: an introduction to weather, climate, and the environment, 5th edn. West Publishing Company, 591 pp

Alexandersson H, Moberg A (1997) Homogenistation of Swedish temperature data. Part I: Homogeneity tet for linear trends. Int J Climatol 17: 25–34

Bacchi B, Kottegoda NT (1995) Identification and calibration of spatial correlation patterns of rainfall. J Hydrol 165(1–4): 311–348

Barry R (1992) Mountain weather and climate, 2nd edn. London: Routledge, 402 pp

Bergström S, Carlsson B, Gardelin M, Lindström G, Petterson A, Rummukainen M (2001) Climate change impacts on runoff in Sweden – assessments by global climate models, dynamical downscaling and hydrological modelling. Clim Res 16: 101–112

Bigg GR (1991) Kriging and intraregional rainfall variability in England. Int J Climatol 11(6): 663–675

Brunsdon C, McClatchey J, Unwin DJ (2001) Spatial variations in the average rainfall-altitude relationship in Great Britain: an approach using geographically weighted regression. Int J Climatol 21: 455–466

Busuioc A, Chen D, Hellström C (2001) Performance of statistical downscaling models in GCM validation and regional climate change estimates: Application for Swedish precipitation. Int J Climatol 21: 557–578

Christensen OB, Christensen JH, Machenhauer B, Botzet M (1998) Very high-resolution regional climate simulations over Scandinavia – Present Climate. J Climate 11: 3204–3229

Christensen JH, Kuhry P (2000) High-resolution regional climate model validation and permafrost simulation for the East European Russian Arctic. J Geophys Res 105(D24): 29647–29658

Clarc I, Harper W (2000) Practical geostatistics 2000. Columbus Ohio: Ecosse North America Llc., 442 pp

Ellesson J (1993) Årsnederbörden i Skåne 1961–90. Svensk Geografisk Årsbok 69: 51–66 (in Swedish)

Frei C, Schär C (1998) A precipitation climatology of the Alps from high-resolution rain-gauge observations. Int J Climatol 18: 873–900

Frich P, Rosenørn S, Madsen H, Jensen JJ (1997) Observed precipitation in Denmark, 1961–90. Technical Report 97–8. DMI, Copenhagen: Danish Meteorological Institute, 40 pp

Giorgio F, Mearns LO (1999) Introduction to special section: Regional climate modeling revisited. J Geophys Res 104: 6335–6352

Hellström C, Chen D, Achberger C, Räisänen J (2001) Comparison of climate change scenarios for Sweden based on statistical and dynamical downscaling of monthly precipitation. Clim Res 19: 45–22

Hellström C, Chen D (2003) Statistical downscaling based on dynamically downscaled predictors: application to monthly precipitation in Sweden. Adv Atmos Sci 20: (in press)

Hu ZZ, Bengtsson L, Roeckner E, Christoph M, Bacher A, Oberhuber JM (2001) Impact of global warming on the interannual and interdecadal climate modes in a coupled GCM. Clim Dyn 17: 361–374

IPCC (2001) Climate Change 2001: The scientific basis. Contribution of Working Group I to the Third Assessment Report of the Intergovernmental Panel on Climate Change. Cambridge, United Kingdom and New York, USA: Cambridge University Press, 881 p

Isaaks EH, Srivastava RM (1989) Applied geostatistics. New York: Oxford University Press, 561 pp

Jacob D (2001) A note to the simulation of the annual and inter-annual variability of the water budget over the Baltic Sea drainage basin. Meteorol Atmos Phys 77: 61–73

Johns TC, Carnell RE, Crossley JF, Gregory JM, Mitchell JFB, Senior CA, Tett SFB, Wood RA (1997) The second Hadley Centre coupled ocean-atmosphere GCM: model description, spinup and validation. Clim Dyn 13: 103–134

Källén E (ed) (1996) HIRLAM documentation manual. System 2.5. 178pp + 55pp appendix (available from SMHI, S-60176 Norrköping, Sweden.)

Lambert SJ, Boer GJ (2001) CMIP1 evaluation and intercomparison of coupled models. Clim Dyn 17: 93–106

Linderson ML (2001) Objective classification of atmospheric circulation over Southern Scandinavia. Int J Climatol 21: 155–169

Linderson ML (2002) Spatial distribution of meso-scale precipitation anomalies in Scania, southern Sweden. Geografiska Annaler (submitted)

Mitchell JFB, Johns TC (1997) On modification of global warming by sulphate aerosols. J Clim 10: 245–267

Mearns LO, Bogardi I, Giorgio F, Matyasovszky I, Palecki M (1999) Comparison of climate change scenarios generated from regional climate model experiments and statistical downscaling. J Geophys Res 104: 6603–6621

Murphy J (1999) An evaluation of statistical and dynamical techniques for downscaling local climate. J Clim 12(8): 2256–2284

New M, Hulme M, Jones P (1999) Representing twentieth-century space-time climate variablity. Part I: Development of a 1961–90 mean monthly terrestrial climatology. J Clim 12(3): 829–856

New M, Hulme M, Jones P (2000) Representing twentieth-century space-time climate variablity. Part II: Development of 1901–96 monthly grids of terrestrial surface climate. J Clim 13(13): 2217–2238

Noguer M, Jones R, Murphy J (1998) Sources of systematic errors in the climatology of a regional climate model over Europe. Clim Dyn 14: 691–712

Oberhuber JM (1993) Simulation of the Atlantic circulation with a coupled sea ice-mixed layer-isopycnal general circulation model. Part I: Model description. J Phys Oceanogr 22: 808–829

Osborn TJ, Hulme M (1997) Development of a relationship between station and gid-box rainday frequencies for climate model evaluation. J Clim 10(8): 1885–1908

Raab B, Vedin H (1995) Climate, lakes and rivers. National Altas of Sweden. Stockholm: SNA Publications, 176 pp

Räisänen J, Joelson R (2001) Changes in average and extreme precipitation in two regional climate model experiments. Tellus 53A: 547–566

Räisänen J, Rummukainen M, Ullerstig A (2001) Downscaling of greenhouse gas induced climate change in two GCMs with the Rossby Centre regional climate model for northern Europe. Tellus 53A: 168–191

Roeckner E, Bengtsson L, Feichter J, Lelieveld J, Rodhe H (1999) Transient climate change simulations with a coupled atmosphere-ocean GCM including the tropospheric sulfur cycle. J Climate 12: 3004–3032

Rubel F, Hantel M (2001) BALTEX 1/6-degree daily precipitation climatology 1996–1998. Meteorol Atmos Phys 77: 155–166

Rummukainen M, Bergström S, Källén E, Moen L, Rodhe J, Tjernström M (2000) SWECLIM – The first three years. SMHI Reports Meteorology and Climatology No. 94. Norrköping, Sweden: Swedish Meteorological and Hydrological Institute, 87 pp

Rummukainen M, Räisänen J, Bringfelt B, Ullerstig A, Omstedt A, Willén U, Hansson U, Jones C (2001) A regional climate model for northern Europe: model description and results from the downscaling of two GCM control simulations. Clim Dyn 17: 339–359

Steffensen P (1996) Standard normal homogeneity test for Windows. User guide. Report no 96:13. Copenhagen: DMI, Danish Meteorological Institute, 33 pp

Taylor KE (2001) Summarizing multiple aspects of model performance in a single diagram. J Geophys Res 106(7): 7183–7192

Wilby RL, Hay LE, Leavesley GH (1999) A comparison of downscaled and raw GCM output: implications for climate change scenarios in the San Juan River basin, Colorado. J Hydrol 225: 67–91

Authors' addresses: Christine Achberger (e-mail: christin@gvc.gu.se), Earth Sciences Centre, Göteborg University, Box 460, 40530 Göteborg, Sweden; Maj-Lena Linderson, Department of Physical Geography and Ecosystems Analysis, Lund University, Sölvegatan 13, 223 62 Lund, Sweden; Deliang Chen, Earth Sciences Centre, Göteborg University, Box 460, 40530 Göteborg, Sweden.